

Optical Spectroscopy of the Somewhat Peculiar Type IIb Supernova 2001ig

JEFFREY M. SILVERMAN,¹ PAOLO MAZZALI,^{2,3} RYAN CHORNOCK,¹ ALEXEI V. FILIPPENKO,¹ ALEJANDRO CLOCCHIATTI,⁴
 MARK M. PHILLIPS,⁵ MOHAN GANESHALINGAM,¹ AND RYAN J. FOLEY^{1,6,7}

Received 2009 March 24; accepted 2009 May 26; published 2009 June 16

ABSTRACT. Here we present previously unpublished optical spectra of supernova (SN) 2001ig, a Type IIb SN, from about a week after explosion until nearly one year later. The earliest spectrum consists of only a few broad absorption features, but soon more common Type II SN features including hydrogen P Cygni profiles and helium absorption become apparent. At later times, as the H features fade and the He I absorption becomes more prominent, we observe the SN to transition from a Type II to a Type Ib. Finally, observations after 250 days past explosion show a nebular-phase SN spectrum with one of the largest magnesium to oxygen intensity ratios ever seen. Additionally, we present models of the late-time spectra which indicate that the inner ejecta consist of $\sim 1.15 M_{\odot}$ of material, most of which (by mass) is in the form of oxygen, with $\sim 0.13 M_{\odot}$ of ^{56}Ni and essentially no hydrogen.

1. INTRODUCTION

It is thought that most high-mass stars ($\gtrsim 8 M_{\odot}$) end their lives as core-collapse supernovae (SNe) (e.g., Woosley & Janka 2005 and references therein). These SNe are divided spectroscopically into subgroups based on the strength of H and He in their optical spectra. The progression from Type II to Ib to Ic corresponds to SNe having both H and He, to just He, to neither H nor He present in their spectra (for a review, see Filippenko 1997). The class of Type IIb SNe (SNe IIb) have spectra that undergo a transition from Type II to Type Ib as their H features fade with time. It is likely that SNe IIb, Ib, and Ic undergo significant mass loss, due either to stellar winds and eruptions or to mass transfer to a binary companion, before explosion.

SN 2001ig was discovered in the nearby late-type spiral galaxy NGC 7424 by Evans et al. (2001) on 2001 December 10.43 (UT dates are used throughout this article). It is located at $\alpha_{J2000} = 22^{\text{h}}57^{\text{m}}30^{\text{s}}.74$ and $\delta_{J2000} = -41^{\circ}02'26''.1$ (Ryder et al. 2001). An explosion date of 2001 December 3 has been estimated by Ryder et al. (2004) from modeling the radio light curve, and we use this as the reference date for our spectral observations throughout this article. A spectrum was obtained within two days of detection of the SN and showed only a few broad absorption features. However, the spectrum from

Las Campanas Observatory on 2001 December 13 (Phillips et al. 2001) revealed similarities to the Type IIb SNe 1987K (Filippenko 1988) and 1993J (Filippenko et al. 1993).

Over the following month, spectra from the European Southern Observatory (Clocchiatti & Prieto 2001; Clocchiatti 2002) showed SN 2001ig to evolve in a manner similar to both SNe IIb 1987K and 1993J, as the hydrogen lines became weaker and showed the complex shape characteristic of the transitional stage (Filippenko et al. 1994). By October 2002, the predicted transition to a Type Ib SN in the nebular phase was complete (Filippenko & Chornock 2002). At the time it was also noted that the Mg I $\lambda 4571$ feature was the strongest (relative to [O I] $\lambda\lambda 6300, 6364$) ever seen in a SN. Our data complement the optical spectropolarimetry and total-flux spectra that were presented and analyzed by Maund et al. (2007b).

In addition to optical data, X-ray images were obtained with the Advanced CCD Imaging Spectrometer-S (ACIS-S) instrument on the *Chandra* X-ray Observatory on 2002 May 22, showing a 0.2–10.0 keV luminosity of $\sim 10^{38} \text{ erg s}^{-1}$ (Schlegel & Ryder 2002). SN 2001ig was also detected at radio frequencies; for further information on the radio data and analysis, see Ryder et al. (2004).

Here we present and analyze optical spectroscopic data as well as two spectral models for SN 2001ig at late times. In § 2 we describe our observations and data reduction, and in § 3 we discuss our analysis of the spectra. Our model spectra and their implications are presented in § 4. We summarize our conclusions in § 5.

2. OBSERVATIONS AND DATA REDUCTION

Beginning one week after explosion, optical spectra were obtained using the LDSS-2 spectrograph (Mulchaey 2001) mounted on the Magellan Baade 6.5 m telescope, the red arm of the dual imager/spectrograph EMMI (Dekker et al.

¹ Department of Astronomy, University of California, Berkeley, CA 94720-3411; JSilverman@astro.berkeley.edu.

² Max-Planck Institut für Astrophysik, Karl-Schwarzschild-Strasse 1, 85748 Garching, Germany.

³ Istituto Naz. di Astrofisica-Oss. Astron., vicolo dell'Osservatorio, 5, 35122 Padova, Italy.

⁴ Pontificia Universidad Católica de Chile, Departamento de Astronomía y Astrofísica, Casilla 306, Santiago 22, Chile.

⁵ Las Campanas Observatory, Casilla 601, La Serena, Chile.

⁶ Harvard-Smithsonian Center for Astrophysics, Cambridge, MA 02138.

⁷ Clay Fellow.

TABLE 1
JOURNAL OF OBSERVATIONS

UT Date	Day ^a	Telescope ^b	Range (Å)	Res. ^c (Å)	Airmass ^d	Exp. (s)
2001 Dec 11	8	LDSS2	3800–9000	13	1.07	2 × 90
2001 Dec 13	10	LDSS2	5000–10000	13	1.18	2 × 60
2001 Dec 16	13	EMMI	3980–9400	9	1.64	3 × 60
2001 Dec 23	20	LRIS	3400–10300	7	2.49	60
2002 Jan 13	41	EFOSC2	3360–10300	9	1.87	3 × 90
2002 Jan 17	45	LRIS	3520–10000	7	4.09	360
2002 Jan 18	46	LRIS	3500–5380	3	4.99	450
2002 Jan 18	46	LRIS	5710–7000	2	4.99	450
2002 Jan 29	57	LDSS2	3600–10000	13	2.61	90
2002 Aug 16 ^e	256	FORS1	4000–8600	12	1.04	4 × 1200
2002 Oct 8	309	LRIS	3150–9420	6	2.18	2 × 600
2002 Nov 8	340	LRIS	3100–9410	6	2.05	900

^a Days since the explosion date of 2001 Dec 3 (estimated by Ryder et al. 2004 from the radio light curve).

^b LDSS2: Magellan Baade 6.5 m/LDSS-2 spectrograph (Mulchaey 2001); EMMI: European Southern Observatory (ESO) 3.6 m New Technology Telescope/red arm of the dual imager/spectrograph EMMI (Dekker et al. 1986); LRIS: Keck I 10 m/Low-Resolution Imaging Spectrometer (Oke et al. 1995); EFOSC2: ESO 3.6 m/dual imager/spectrograph EFOSC2 (Buzzoni et al. 1984); FORS1: ESO 8.2 m Very Large Telescope/FORS1 spectrograph (Appenzeller et al. 1998).

^c Approximate spectral resolution.

^d Airmass at midpoint of exposures.

^e Spectrum previously published by Maund et al. (2007b).

1986) mounted on the European Southern Observatory (ESO) 3.6 m New Technology Telescope, the Low-Resolution Imaging Spectrometer (LRIS; Oke et al. 1995) mounted on the Keck I 10 m telescope, and the dual imager/spectrograph EFOSC2 (Buzzoni et al. 1984) mounted on the ESO 3.6 m telescope. Our last spectral observation occurred on 2002 November 8, approximately 340 days after explosion. All observations used a 0.7"–1.0" wide slit and were aligned along the parallactic angle to reduce differential light losses (Filippenko 1982). Table 1 summarizes the spectral data of SN 2001ig presented in this article.

All spectra were reduced using standard techniques (e.g., Foley et al. 2003). Standard CCD processing and spectrum extraction for the LRIS data were completed with IRAF⁸, and the data were extracted with the optimal algorithm of Horne (1986). We obtained the wavelength scale from low-order polynomial fits to calibration-lamp spectra. Small wavelength shifts were then applied to the LRIS data after cross-correlating a template sky to the night-sky lines that were extracted with the SN. Using our own IDL routines, we fit spectrophotometric standard-star spectra to the LRIS data in order to flux calibrate our spectra and to remove telluric lines (Wade & Horne 1988; Matheson et al. 2000).

⁸ IRAF: the Image Reduction and Analysis Facility is distributed by the National Optical Astronomy Observatory, which is operated by the Association of Universities for Research in Astronomy (AURA) under cooperative agreement with the National Science Foundation.

Each EMMI observation was reduced independently and the final spectra were combined with a pixel-rejection algorithm based on the mean.

3. SPECTRAL ANALYSIS

3.1. Early-Time Spectra

We present our early-time spectra of SN 2001ig in Figure 1; all have had the recession velocity of NGC 7424 removed (939 km s^{−1}, from Koribalski et al. 2004). The first spectrum of SN 2001ig, taken on 2001 December 11 (8 days past explosion), shows only a few strong, broad absorption features. We conjecture that the feature near 4000 Å is Hγ and the feature near 4300 Å is a blend of Fe II lines (near a rest wavelength of 4570 Å) blueshifted by ~22,500 km s^{−1} and ~18,200 km s^{−1}, respectively. Unfortunately, this identification is somewhat dubious since the Hγ feature appears to be unusually strong.

Instead, we note that this pair of features resembles the “W” feature seen in very early-time spectra of the Type II SN 2005ap (Quimby et al. 2007) and the Type Ib SN 2008D (Malesani et al. 2009; Modjaz et al. 2009, a spectrum of which is reproduced in Figure 1). The features in both objects were attributed to a combination of C III, N III, and O III at blueshifted velocities of ~21,000 km s^{−1} and ~30,000 km s^{−1}, respectively. If we assume that these are the correct line identifications, then they are blueshifted by ~26,000 km s^{−1} in the day 8 spectrum of SN 2001ig. However, there is some uncertainty in the bluer of these two features since its left wing is distorted somewhat by the

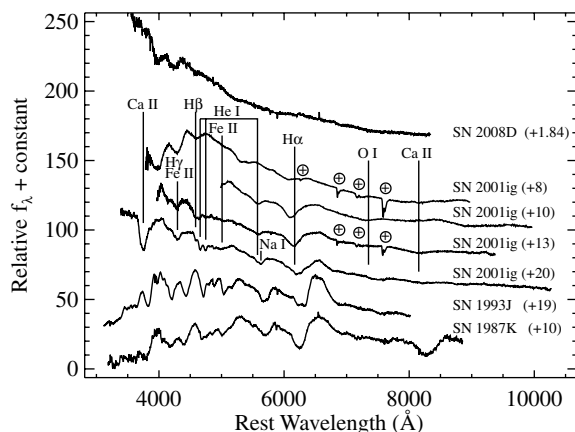


FIG. 1.—Spectra of SN 2001ig (and three comparison SNe) with some line identifications. The top spectrum is SN 2008D (Modjaz et al. 2009) and has been dereddened by $E(B - V)_{\text{Host}} = 0.6$ mag. The next four spectra, of SN 2001ig, from top to bottom were obtained on 2001 Dec 11, 13, 16, and 23; ages shown are relative to the adopted explosion date of 2001 Dec 3. The bottom two spectra are SN 1993J (Filippenko et al. 1994) and SN 1987K (Filippenko 1988). Recession velocities of 2100 km s^{-1} (Modjaz et al. 2009), 939 km s^{-1} (Koribalski et al. 2004), -34 km s^{-1} , and 805 km s^{-1} (both from de Vaucouleurs et al. 1991) have been removed from the spectra of SNe 2008D, 2001ig, 1993J, and 1987K, respectively. Telluric features are indicated by the \oplus symbol.

noise at the bluest end of our spectrum. It should also be noted that Mazzali et al. (2008) found no evidence for the “W” feature in their earliest spectrum of SN 2008D.

The third feature (near 4600 \AA) can be decomposed into two Gaussian profiles centered at $\sim 4498 \text{ \AA}$ and $\sim 4596 \text{ \AA}$, which could be a blend of $\text{H}\beta$ and $\text{He I } \lambda\lambda 4921, 5015$ blueshifted by $\sim 23,200 \text{ km s}^{-1}$ and $\sim 23,300 \text{ km s}^{-1}$, respectively. At this epoch SN 2001ig defies simple classification (as pointed out by Phillips et al. 2001).

There is also weak, but broad, absorption at $\sim 5300 \text{ \AA}$ and 5420 \AA , the latter of which could be $\text{He I } \lambda 5876$ blueshifted by $\sim 24,100 \text{ km s}^{-1}$. In addition, the absorption near 6060 \AA is most likely $\text{H}\alpha$ blueshifted by $\sim 24,000 \text{ km s}^{-1}$.

We measure a blackbody-fit temperature of $\sim 14,000 \text{ K}$ for the continuum of this observation. In comparison, the derived early-time blackbody temperatures of SNe 1993J and 2008D were $\sim 12,000 \text{ K}$ (Clocchiatti et al. 1995) and $13,000 \text{ K}$ (Modjaz et al. 2009), respectively, which match nicely with SN 2001ig.

In our highest-resolution spectrum, taken on 2002 January 18 (46 days after explosion; see § 3.2 for more on this observation), we measure an upper limit to the equivalent width (EW) of the Na I D line in NGC 7424 of $\sim 0.1 \text{ \AA}$. This corresponds to a host-galaxy reddening of $E(B - V) \lesssim 0.02$ mag (Munari & Zwitter 1997), which is comparable to the Galactic reddening of $E(B - V) = 0.011$ mag from Schlegel et al. (1998). The low host reddening for SN 2001ig is reasonable since the SN occurred on the outskirts of the galaxy. Since these numbers are both quite small, we ignore reddening when plotting our

spectra. We also note that Maund et al. (2007b) required a total reddening somewhat in excess of the Galactic value plus the value we calculate for the host to explain the polarization they observe.

In all other early-time spectra, we detect $\text{He I } \lambda 5876$ and P Cygni profiles of $\text{H}\alpha$ (with the absorption component greatly dominating over the emission component). The observation from 2001 December 13, for example, shows the He I feature blueshifted by $\sim 16,000 \text{ km s}^{-1}$. In addition, Phillips et al. (2001) mention that there are broad absorption features at 4080 \AA and 4580 \AA in the observation from 2001 December 13, and it is possible that they are $\text{H}\gamma$ and $\text{H}\beta$, respectively. However, the observation lacked acceptable blue-side flatfields and proper wavelength-calibration files, so data at wavelengths $\lesssim 5000 \text{ \AA}$ cannot be completely trusted. We also identify the very weak, broad absorption near 7300 \AA as $\text{O I } \lambda 7774$.

By 13 days after the explosion, many more spectral features have appeared. Still present are the P Cygni profile of $\text{H}\alpha$ and the $\text{He I } \lambda 5876$ line. Maund et al. (2007b) point out that $\text{H}\alpha$ at this time is likely to be blended with $\text{He I } \lambda 6678$. No longer visible in this spectrum is the aforementioned “W” feature that probably came from a combination of C III, N III, and O III. This is again similar to SN 2008D, whose “W” disappeared in the span of ~ 1 day (Modjaz et al. 2009). However, there are still features at about 4130 \AA and 4287 \AA , and we associate these with possible absorption due to $\text{H}\gamma$ and Fe II , respectively.

The feature near 4600 \AA is most likely $\text{H}\beta$ while the noisy dips just below 4800 \AA are probably due to a combination of $\text{He I } \lambda\lambda 4921, 5015$ and $\text{Fe II } \lambda\lambda 4924, 5018$. Also seen is weak absorption likely due to $\text{Fe II } \lambda 5169$ near 5030 \AA and quite broad, weak absorption from the Ca II near-infrared (IR) triplet around 8150 \AA .

On 2001 December 23, we acquired the fifth spectrum from the top of Figure 1. Again, we detect the $\text{H}\alpha$ P Cygni line, although now it has a far more complex profile with a larger full width at half-maximum intensity (FWHM) than previously seen. This implies that the $\text{H}\alpha$ feature is now likely becoming blended with $\text{Si II } \lambda 6355$. The feature near 5600 \AA in this spectrum clearly shows two local minima which are probably due to $\text{He I } \lambda 5876$ and Na I D . Also in this observation we detect distinct $\text{H}\beta$, $\text{He I } \lambda 4921$, and $\text{He I } \lambda 5015$ absorption, in addition to absorption from the Ca II near-IR triplet around 8200 \AA . Finally, extremely strong absorption due to Ca II H and K lines can now be seen near 3750 \AA .

It has been pointed out that, in many ways, the first few spectra of SN 2001ig resemble those of SNe 1987K and 1993J at early times (Phillips et al. 2001; Clocchiatti & Prieto 2001). Examples of both at similar ages are plotted for comparison in Figure 1 and there do appear to be quite a few similarities among these objects. However, it should be noted that $\text{H}\alpha$ (both the absorption and emission components) is weaker in SN 2001ig. In addition, the overall continuum shape of SN 2001ig does not change much during this two-week period.

Figure 1 also indicates that SN 2001ig has a bluer continuum than either SN 1987K or SN 1993J; however, this could be due to reddening. Both SNe 1987K and 1993J are plotted with no reddening correction, which is approximately consistent with observations (Richmond et al. 1994), but there is also evidence that the color excess of SN 1993J is as high as 0.25–0.32 mag (Richmond et al. 1994; Clocchiatti et al. 1995).

3.2. Transition Spectra

Our spectra from ~ 5.5 weeks past explosion to ~ 8 weeks past explosion are presented in Figure 2. The most obvious change in the spectra of SN 2001ig from Figure 1 to Figure 2 is that the flux in the blue part of the continuum has decreased significantly; SN 2001ig now looks very much like SN 1993J in its overall continuum shape. In addition, SNe 2001ig and 1993J look closely similar in the range ~ 4000 – 6000 Å, much of which is a forest of Fe II blends (with some hydrogen Balmer and He I lines as well). As noted by Clocchiatti (2002), the main difference at this time between SNe 2001ig and 1993J is that SN 2001ig has stronger Ca II H and K lines, weaker H I and He I lines, and faster expansion velocities.

Also mentioned by Clocchiatti (2002), by 2002 January 13 (the top spectrum in Fig. 2), SN 2001ig has begun its transition from Type II to Type Ib. This transformation is marked by the decrease in strength of H α and H β while the He I spectral features increase in strength. The most notable cases of this are the dramatic appearances of the He I $\lambda 6678$ absorption feature, which appears as a notch on the red wing of the H α absorption profile, and strong He I $\lambda 7065$ absorption, which unfortunately coincides with a telluric absorption band in the day 41 and 57 spectra. This transformation continues during the subsequent

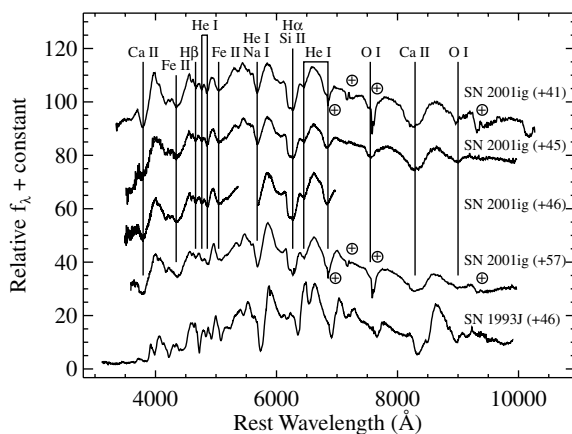


Fig. 2.—Spectra of SN 2001ig (and a comparison SN Iib) with some line identifications. From top to bottom, the spectra were obtained on 2002 Jan 13, 17, 18, and 29; ages shown are relative to the adopted explosion date of 2001 Dec 3. The bottom spectrum is SN 1993J (Filippenko et al. 1994). Recession velocities have been removed from the spectra. Telluric features are indicated by the \oplus symbol.

two weeks of observations (i.e., the rest of the SN 2001ig spectra in Fig. 2).

The minimum of the H α absorption feature is becoming more complex and appears to have developed a double-troughed profile. This is to be expected since at this time H α is being heavily blended with Si II $\lambda 6355$. In addition, as was pointed out by Maund et al. (2007b), the He I $\lambda 5876$ feature has become more prominent and the red wing of its absorption now shows a notch due to Na I D absorption.

Also, by this time the Ca II H and K feature has developed a P Cygni profile with quite a strong emission component. In addition, the Ca II near-IR triplet absorption has strengthened dramatically. The previously identified absorption from Fe II near 4300 Å and 5000 Å becomes stronger, broader, and more complex with time. This is likely due to line blanketing, which was also seen in SN 2002ap (Foley et al. 2003).

The broad absorption near 9000 Å could be O I $\lambda 9266$ at about -9000 km s $^{-1}$. In addition, strong, relatively broad absorption from O I $\lambda 7774$ is again seen in these observations, but at roughly -8000 km s $^{-1}$. However, this feature coincides with a telluric absorption band in the day 41 and 57 spectra, making the velocity determination difficult and uncertain.

3.3. Late-Time Spectra

A late-time spectrum from Maund et al. (2007b) (256 days past explosion) and our late-time spectra (309 and 340 days past explosion) are presented in Figure 3 and are compared with similar late-time spectra of SNe 1993J and 2002ap. SN 2001ig has reached the nebular phase by this time and has quite strong [O I] $\lambda\lambda 6300, 6364$ and Mg I $\lambda 4571$ emission. These and other common nebular SN features are marked in Figure 3; the

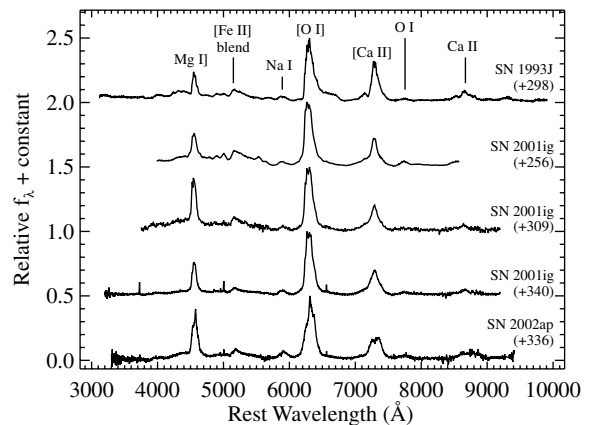


Fig. 3.—Spectra of SN 2001ig (and two comparison SNe) with some line identifications. The top spectrum is SN 1993J (Filippenko et al. 1994). The next three spectra are SN 2001ig and were obtained on 2002 Aug. 16 (from Maund et al. 2007b, Fig. 2, reproduced with permission), Oct 8, and Nov 8; ages shown are relative to the adopted explosion date of 2001 Dec 3. The bottom spectrum is the Type Ic SN 2002ap (Foley et al. 2003). Recession velocities have been removed from the spectra (657 km s $^{-1}$ for SN 2002ap, from Lu et al. 1993).

features of SNe 2001ig, 2002ap, and 1993J are all similar, but the relative strengths of some of the emission lines differ.

One of the most notable differences among the objects is that SN 1993J exhibits obvious $H\alpha$ emission by day 298, appearing as a shoulder on the red wing of $[O\text{ I}] \lambda\lambda 6300, 6364$. Filippenko et al. (1994) and Matheson et al. (2000) showed that the $H\alpha$ feature gradually strengthened from this time onward in SN 1993J, whereas in spectra at similar epochs of SN 2001ig shown in Figure 3 there is no obvious $H\alpha$ emission. For SN 1993J, the hydrogen at late times was attributed to interaction with circumstellar gas, but in SN 2001ig, we see no evidence for such an interaction.

Figure 3 also shows that the blended $[\text{Fe II}]$ emission near 5200 \AA is weak, which indicates a relatively small ^{56}Ni mass (see § 4 for more information on the mass of the ejecta). The line profiles of $\text{Mg I } \lambda 4571$, $[\text{O I}] \lambda\lambda 6300, 6364$, and $[\text{Ca II}] \lambda\lambda 7291, 7324$ in the spectra of SN 2001ig in Figure 3 are quite strong and complex; Figure 4 illustrates them in detail. The Mg I and $[\text{O I}]$ lines at all epochs appear to have a broad peak, punctuated by multiple local maxima. Mg I has peaks

near -2000 km s^{-1} and at -1000 km s^{-1} relative to the systemic velocity of NGC 7424 (939 km s^{-1} ; Koribalski et al. 2004). This line may also have another bump near -3000 km s^{-1} in the blue wing of the main feature. The $[\text{O I}]$ emission is even more complex, with local peaks near -3000 km s^{-1} , -1700 km s^{-1} , 150 km s^{-1} , and 1200 km s^{-1} (again relative to the systemic velocity of NGC 7424). The $[\text{Ca II}] \lambda\lambda 7291, 7324$ emission in Figure 4 has a broad peak which is blueshifted by $\sim 1000 \text{ km s}^{-1}$ in all three epochs.

Figure 4 also shows the temporal evolution of the $\text{Mg I } \lambda 4571$ and $[\text{O I}] \lambda\lambda 6300, 6364$ line profiles. One of the most notable changes is the decrease in relative flux in the far wings of the Mg I line near $\pm 5000 \text{ km s}^{-1}$. As mentioned, the feature near -3000 km s^{-1} appears to decrease in strength with time. This decrease of relative flux with time near -3000 km s^{-1} is also seen in the $[\text{O I}]$ feature. Finally, we note that there is also an increase in the flux in the wings of the $[\text{Ca II}]$ feature near $\pm 2000\text{--}5000 \text{ km s}^{-1}$.

The complex structure of the $\text{Mg I } \lambda 4571$ and $[\text{O I}] \lambda\lambda 6300, 6364$ lines has been seen previously in another well-studied Type IIB, SN 1993J (Matheson et al. 2000). They found that the $[\text{O I}]$ and Mg I line profiles resulted from clumps in the ejecta while the $[\text{Ca II}]$ lines did not. They also pointed out that this is consistent with the explosion scenario first proposed for SN 1987A by Li & McCray (1992, 1993), in which the emission from oxygen comes from clumps of newly synthesized material while the calcium emission originates mainly in preexisting uniformly distributed material. Filippenko & Sargent (1989) found similar irregularities in the $[\text{O I}] \lambda\lambda 6300, 6364$ lines of the SN Ib 1985F. They suggested that the spectral peculiarities come either from Rayleigh-Taylor fingers of higher-speed material or from local density enhancements.

The $[\text{O I}]$ doublet of SN 2001ig somewhat resembles that of the peculiar SN Ib 2005bf (Modjaz et al. 2008) in that SN 2001ig may also show a double-peaked profile with one of the peaks near zero velocity and the other blueshifted by a few thousand km s^{-1} . However, the Mg I line in SN 2001ig at all epochs has a broad profile with a complex top and does not seem to exhibit the same double-peaked nature of the $[\text{O I}]$ emission. This differs from the results of Foley et al. (2003) for the energetic broad-lined SN Ic 2002ap, which showed identical $[\text{O I}]$ and Mg I profiles. In addition, the flux in the Mg I line appears to be more centrally concentrated in SN 2001ig compared to SN 2002ap.

It has been proposed that the double-peaked $[\text{O I}]$ profile of SN 2005bf was caused by a unipolar blob or jet (Maeda et al. 2007) while its polarization signature was attributed to a possible “tilted jet” passing through an asymmetric photosphere (Maund et al. 2007a, 2007b). Both our models of late-time spectra of SN 2001ig and the similarity of the profiles in our late-time spectra to those of SN 1993J (Matheson et al. 2000) indicate clumpy, oxygen-rich ejecta as well (see § 4 for more information regarding the models and ejecta). Thus,

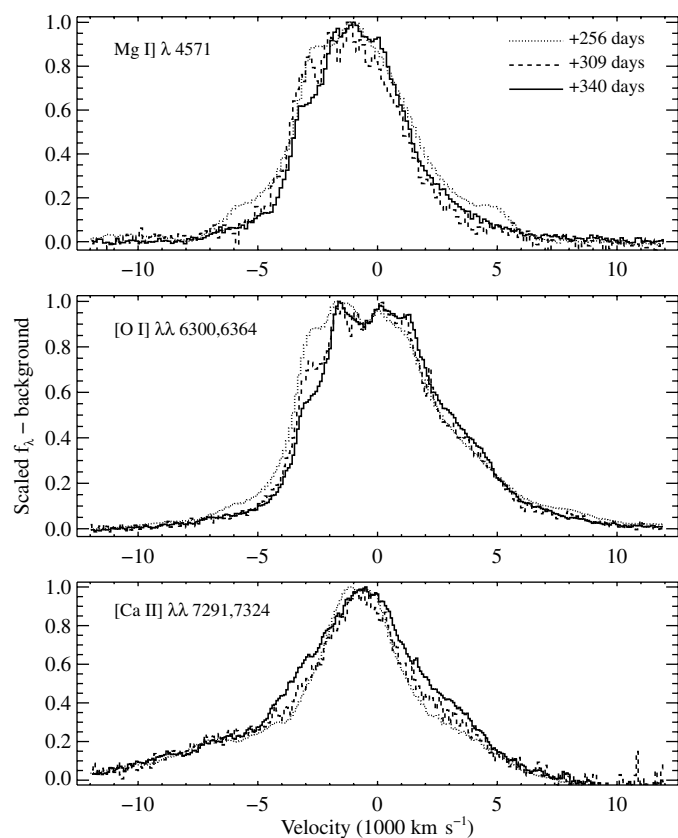


FIG. 4.—The profiles of $\text{Mg I } \lambda 4571$ (top), $[\text{O I}] \lambda\lambda 6300, 6364$ (middle), and $[\text{Ca II}] \lambda\lambda 7291, 7324$ (bottom) in SN 2001ig at three epochs, relative to the systemic velocity of the host galaxy NGC 7424. Ages relative to the adopted explosion date of 2001 Dec 3 are shown. To create these figures, a local linear background was subtracted from each feature and the maxima of the features were all scaled to 1.0.

SN 2001ig probably has large-scale asymmetry in its ejected oxygen, either in the form of a blob or jet (tilted or otherwise), while the distributions of magnesium and calcium appear more uniform (though the magnesium seems only marginally more uniform than the oxygen). This is supported by Fransson & Chevalier (1989), who predicted that magnesium and calcium should be found closer to the core of the explosion than oxygen.

Filippenko & Chornock (2002) stated that the Mg I] $\lambda 4571$ feature was the strongest (relative to [O I] $\lambda\lambda 6300, 6364$) ever seen in a SN. We investigate this claim more closely and the results are shown in Table 2, where we list the relative line strengths for each nebular spectrum of SN 2001ig along with some of the values from Foley et al. (2003, Table 6) and values calculated from other SN spectra in the literature. To compute the relative line strengths for SN 2001ig, we subtracted a local continuum from each spectral feature and then integrated the flux in each line. This is the same procedure presented by Foley et al. (2003).

Although it has been pointed out that this method of line-strength measurement is somewhat inaccurate (Foley et al. 2003), it does seem to indicate that the Mg I] line of SN 2001ig grows with time with respect to the [Ca II] $\lambda\lambda 7291, 7324$ doublet and the [O I] doublet. Relative to the [Ca II] feature, the Mg I] emission from SN 2001ig is somewhat weaker than that of SN 2002ap at similar epochs. The other SNe that also appeared in Foley et al. (2003, Table 6) all have about the same Mg I] strength, which is lower than that of either SNe 2001ig or 2002ap. However, we also perform this measurement on a few SNe from the literature (see Table 2) and find that while

SNe 2008D (Modjaz et al. 2009) and 1993J (Matheson et al. 2000) have comparable Mg I] strength, this feature is quite strong in the broad-lined Type Ic (Ic-BL) SNe 2006aj (Mazzali et al. 2007a) and 2003jd (Valenti et al. 2008).

Again comparing SN 2001ig to the SNe that appeared in Foley et al. (2003, their Table 6), it has a Mg/O ratio comparable to that of SNe 1994I and 2002ap, but larger than that of SNe 1998bw and 1985F. In addition, the Mg/O ratio of SN 2001ig is similar to that of SNe 2008D, 2006aj, and 2003jd (which in fact has quite a large ratio), but significantly greater than that of SN 1993J. This confirms the claim of Filippenko & Chornock (2002) that SN 2001ig had the strongest nebular O/Mg emission-line ratio of any SN observed at that time. Table 2 also seems to indicate that it is not uncommon for core-collapse SNe to have relatively large Mg/O ratios, yet what distinguishes between the SNe that do or do not show this is unclear.

4. SPECTRAL MODELS

By several months after the explosion of a SN, the densities in the ejecta are sufficiently low from expansion that the opacity drops below unity and the gas obeys nebular physics. At this time it is heated by radioactive decay of ^{56}Ni and cooled by line emission. The resulting line profiles map rather directly the distribution of the heating material and can be used to derive several properties including ^{56}Ni mass, mass of the emitting elements, and morphology of the explosion (Mazzali et al. 2005).

In order to derive accurate models, we need our spectra to be as spectrophotometrically well calibrated as possible. While the relative fluxes of our data are accurate because of our

TABLE 2
INTEGRATED FLUXES RELATIVE TO [Ca II] $\lambda\lambda 7291, 7324$

Supernova	Day ^a	Mg I] 4571 Å	[O I] 6300, 6364 Å	Ca II near-IR 8498, 8542, 8662 Å	Mg/O Ratio
SN 2001ig(IIb) ^b	256	0.38	1.77	... ^c	0.21
SN 2001ig(IIb)	309	0.74	2.06	0.30	0.36
SN 2001ig(IIb)	340	0.83	1.99	0.57	0.42
SN 2008D (Ib) ^d	109	0.34	1.02	5.61	0.33
SN 2006aj (Ic-BL) ^e	153	1.19	4.39	1.37	0.27
SN 2003jd (Ic-BL) ^f	367	0.73	1.58	0.80	0.46
SN 1993J (IIb) ^g	298	0.27	1.79	0.36	0.15
SN 2002ap (Ic) ^h	242	0.72	2.17	0.91	0.33
SN 2002ap (Ic) ^h	274	0.63	2.01	0.66	0.31
SN 2002ap (Ic) ^h	336	1.00	2.29	0.45	0.43
SN 2002ap (Ic) ^h	386	0.87	2.19	0.46	0.40
SN 1998bw (Ic) ^h	215	0.23	1.47	0.41	0.15
SN 1994I (Ic) ^h	146	0.26	0.97	0.84	0.26
SN 1985F (Ib/c) ^h	~240	0.26	3.15	0.56	0.08

^a Days since explosion.

^b Spectrum previously published by Maund et al. (2007b).

^c Spectrum ends at 8600 Å.

^d Spectrum previously published by Modjaz et al. (2009).

^e Spectrum previously published by Mazzali et al. (2007a).

^f Spectrum previously published by Valenti et al. (2008).

^g Spectrum previously published by Filippenko et al. (1994).

^h Values from Foley et al. (2003, their Table 6).

flux-calibration routines (see § 2), the absolute fluxes may be off due to imperfect observing conditions. To address this, we obtained publicly available photometric data on SN 2001ig from ESO and the Space Telescope–European Coordinating Facility (ST-ECF) Science Archive Facility⁹. The observations were single 60 s Bessell (Bessell 1990) *R*-band images taken with the FORS1 spectrograph mounted on the ESO 8.2 m Very Large Telescopes Melipal and Antu (Appenzeller et al. 1998).

We calibrated both images, observed on 2002 October 12 and 2002 December 8, to the United States Naval Observatory B1.0 (USNOB) Catalog with three comparison stars and measured magnitudes for SN 2001ig of 17.99 ± 0.08 and 19.13 ± 0.14 , respectively. In addition to our stated statistical uncertainty, we adopt a systematic uncertainty of ~ 0.25 mag based on comparisons of USNOB magnitudes to Bessell *R*-band magnitudes obtained as part of the Lick Observatory Supernova Search (LOSS; Filippenko et al. 2001) photometry follow-up program. We then synthesized Bessell *R*-band magnitudes from our late-time spectra (taken on 2002 October 8 and 2002 November 8) and compared them to the magnitudes derived from the photometry, assuming a linear decline in magnitude during the last three months of 2002. In order for our spectra to match the photometry, and thus for the absolute flux to be accurate, our spectra from 2002 October 8 and 2002 November 8 must be scaled up by factors of 4.41 and 1.29, respectively. Due to the photometric measurements alone, the uncertainty in the absolute flux of each of these two spectra is $\sim 25\%$.

We modeled both late-time spectra of SN 2001ig using a code that computes nebular-line emission from a gaseous cloud. The gas is heated by the deposition of γ -rays and positrons produced by the decay of radioactive ^{56}Ni (which is produced in the SN explosion itself) into ^{56}Co and then into stable ^{56}Fe . The energy thus deposited in the gas is thermalized collisionally, which leads to excitation and ionization of the gas. Heating is balanced by cooling, which takes place via line emission. Most of the emission lines are forbidden, but some permitted transitions (e.g., the Ca II near-IR triplet) are also active. The code is based on the original description by Axelrod (1980). The propagation of the γ -rays is followed with a Monte Carlo procedure (Cappellaro et al. 1997). Level populations are computed assuming nonlocal thermodynamic equilibrium (non-LTE). A more detailed description is provided by Mazzali et al. (2007b).

Modeling the spectra also requires knowledge of the reddening of, and distance to, the SN. As discussed in § 3.1, the reddening within NGC 7424 is negligible and we have only an upper limit from our data, so we adopt a total reddening of $E(B - V) = 0.011$ mag from Schlegel et al. (1998) for the models. For the distance to SN 2001ig we have used a recession

velocity of 939 km s^{-1} ($z = 0.003132$; Koribalski et al. 2004) throughout this article, yielding a distance modulus of $m - M = 30.5$ mag with $H_0 = 73 \text{ km s}^{-1} \text{ Mpc}^{-1}$ (Riess et al. 2005), assuming that the entire recession velocity is due to the Hubble flow. However, there is some uncertainty in this value due to the relatively small distance to NGC 7424. A search of the literature reveals a range in distance moduli for this galaxy of $30.2\text{--}30.7$ mag using various independent techniques (HyperLEDA¹⁰; Tully 1988; Mould et al. 2000; Meurer et al. 2006; Davis, M., 2009, private communication¹¹). The value of 30.5 mag that we use here is a reasonable average as long as we keep in mind that it has an uncertainty of ~ 0.3 mag which leads to an uncertainty of $\sim 30\%$ in the absolute flux of each late-time spectrum. When this is combined in quadrature with the uncertainty from the photometric measurements, the total uncertainty in the absolute flux of each of our late-time spectra is $\sim 39\%$.

The late-time spectra and models are shown in Figure 5; both models appear to fairly accurately reproduce the major features observed in the data. However, the emission near 4000 \AA and the O I feature near 7700 \AA seem somewhat suppressed in the models. In addition, the intensity of the Ca II feature near 8600 \AA in the models is somewhat larger than that of the observed spectrum, leading to a small inconsistency in the position of the combined Ca II plus [C I] $\lambda 8727$ emission.

Here we use the one-zone version of the model described by Mazzali et al. (2007b). It requires an emitting nebula with an outer velocity of 4300 km s^{-1} , as determined from reproducing the width of the strongest emission lines ([O I], Mg I, and [Ca II]). The spectrum is powered by $\sim 0.13 M_\odot$ of ^{56}Ni . This is determined from the combination of the intensity of the [Fe II] emission feature near 5200 \AA and the requirement that the energy emitted in the radioactive decay chain of ^{56}Ni excites other ions and reproduces the observed emission in other lines. This is a slightly larger value than what was derived for SN 1993J (see Swartz et al. 1993 and references therein), but it is still fairly typical for core-collapse SNe.

The total mass enclosed within the outer velocity of 4300 km s^{-1} is $\sim 1.15 M_\odot$. Interestingly, our models of SN 2001ig are quite similar to that of the SN Ic 1994I which underwent significant mass loss, most likely in a binary interaction, and which also ejected $\sim 1 M_\odot$ of material (Sauer et al. 2006). Nomoto et al. (1994) showed the progenitor star of SN 1994I to be $\sim 15 M_\odot$ initially, which suggests that the progenitor of SN 2001ig was also initially $\sim 15 M_\odot$.

Furthermore, Van Dyk et al. (2002) and Maund et al. (2004) found that both the companion and the progenitor of SN 1993J had initial masses of $\sim 15 M_\odot$ and that the companion of SN 1993J is currently $22 M_\odot$. Ryder et al. (2006) discovered that

¹⁰ See <http://leda.univ-lyon1.fr/>.

¹¹ Using the 2MASS Redshift Survey (2MRS) galaxy catalog to model bulk flows in the local Universe.

⁹ See <http://archive.eso.org/>.

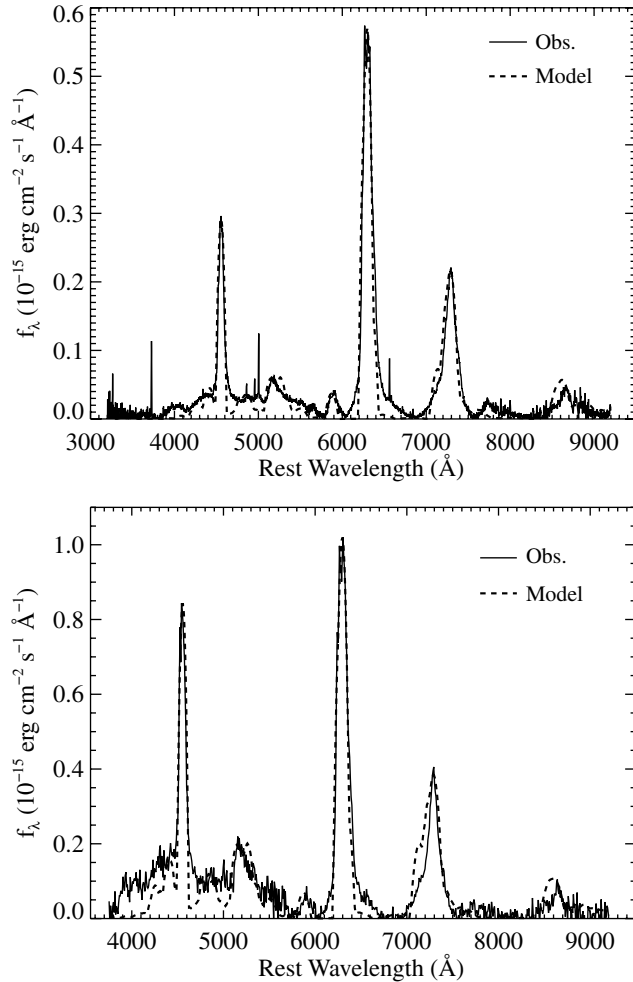


FIG. 5.—The model and observed spectra of SN 2001ig from 2002 Oct 8 (309 days after explosion, *top*) and 2002 Nov 8 (340 days after explosion, *bottom*). The recession velocity of the host galaxy NGC 7427 has been removed from the spectra. The model accurately reproduces the major spectral features seen in the data.

the companion of SN 2001ig is currently $10\text{--}18 M_{\odot}$, so it seems likely that the progenitors of SN 2001ig and SN 1993J (and possibly even SN 1994I) had similar initial masses, and that their companions have similar masses as well. The differences in the companions' masses (as well as physical separations from the progenitors) probably led to slightly different mass-loss and interaction histories which gave rise to the spectroscopic differences observed.

Table 3 shows the complete mass composition of the models. The upper and lower error bars represent the change in the derived abundance after increasing and decreasing the measured flux by 39% to reflect the flux-calibration uncertainties mentioned above. As in the nebular spectra of all other stripped-envelope SNe, and unlike the case in SNe Ia, [Fe III] lines are missing (in particular a strong feature near 4800 \AA). This is best reproduced by assuming fairly significant clumping in

TABLE 3
MASS COMPOSITION OF THE MODELS^a

Element	Mass (M_{\odot}) Day 309	Mass (M_{\odot}) Day 340
C	$2.0^{+0.0}_{-0.8} \times 10^{-2}$	$5.0^{+0.0}_{-1.0} \times 10^{-2}$
O	$8.1^{+2.0}_{-2.1} \times 10^{-1}$	$8.2^{+1.8}_{-1.7} \times 10^{-1}$
Na	$7.0^{+0.0}_{-1.5} \times 10^{-5}$	$1.0^{+0.2}_{-0.0} \times 10^{-4}$
Mg	$1.1^{+0.2}_{-0.0} \times 10^{-2}$	$1.1^{+0.2}_{-0.0} \times 10^{-2}$
Si	$1.0^{+0.0}_{-0.0} \times 10^{-1}$	$1.0^{+0.0}_{-0.0} \times 10^{-1}$
S	$3.0^{+0.0}_{-0.0} \times 10^{-2}$	$3.0^{+0.0}_{-0.0} \times 10^{-2}$
Ca	$3.1^{+0.8}_{-0.9} \times 10^{-2}$	$4.0^{+1.2}_{-0.9} \times 10^{-2}$
⁵⁶ Ni	$1.5^{+0.3}_{-0.3} \times 10^{-1}$	$1.1^{+0.2}_{-0.3} \times 10^{-1}$
Total	$1.2^{+0.3}_{-0.3}$	$1.2^{+0.2}_{-0.2}$

^a The upper and lower error bars represent the change in the derived abundance after increasing and decreasing the measured flux by 39% to reflect the flux-calibration uncertainties mentioned in § 4.

the ejecta, which is a signature of an aspherical explosion (e.g., Mazzali et al. 2007b). Maund et al. (2007b) use spectropolarimetric observations of SN 2001ig to come to the same conclusion regarding the asphericity.

The dominant element in the ejecta by mass is oxygen ($0.81 M_{\odot}$). The derived carbon abundance is quite small ($0.04 M_{\odot}$); otherwise, the emission near 8500 \AA would become too strong. We point out that a small C/O ratio is not unusual in stripped-envelope SNe. In addition, hydrogen may be present only marginally at these low velocities, as deduced from the almost complete absence of any emission (as seen in Fig. 3).

As mentioned in § 3.3, the late-time spectra of SN 2001ig have an unusually large Mg/O intensity ratio, comparable to that of SN 2002ap. However, the Mg/O ratio by mass of SN 2001ig is ~ 0.014 (see Table 3) while that of SN 2002ap is ~ 0.032 (Mazzali et al. 2007b). This difference in masses is consistent with the fact that the envelope of SN 2002ap was extremely stripped before explosion, since it showed no spectroscopic evidence of hydrogen or helium (Foley et al. 2003). On the other hand, the envelope of SN 2001ig was only partially stripped prior to core collapse, since we observed a significant amount of hydrogen and helium at early times.

5. CONCLUSIONS

In this article we have presented and analyzed optical spectra of SN 2001ig. One week after explosion, the SN defied simple spectral classification, but by two weeks after explosion SN 2001ig appeared to be part of the Type IIb subclass of SNe. This was confirmed as the SN went through a transition from Type II to Type Ib during the first few months of observations.

By nine months after explosion, SN 2001ig had entered the nebular phase, revealing some of the strongest Mg I] $\lambda 4571$ and [O I] $\lambda \lambda 6300, 6364$ features ever observed in a SN; its Mg/O intensity ratio is one of the largest ever seen as well.

We derive models of SN 2001ig from our spectra taken 309 and 340 days after the explosion, showing that the majority of the inner ejecta (below 4300 km s^{-1}) were in the form of

oxygen, and a significant fraction (nearly $0.13 M_{\odot}$) in the form of ^{56}Ni . Additionally, there appears to be a distinct lack of hydrogen in the inner ejecta. We also find that the total mass of this inner ejecta was $\sim 1.15 M_{\odot}$, suggesting that the progenitor of SN 2001ig was a relatively low-mass star ($\sim 15 M_{\odot}$).

We are grateful to the staffs at the Keck Observatory, ESO, and Las Campanas Observatory for their support. We thank the following for their assistance with some of the observations and data reduction: F. Barrientos, R. Carlberg, M. Gladders, S. W. Jha, T. Matheson, J. L. Prieto, and B. Leibundgut. We especially thank J. Maund and his collaborators for allowing us to reproduce one of their spectra. Some of the data presented herein were obtained at the W. M. Keck Observatory, which is operated as a scientific partnership among the California

Institute of Technology, the University of California, and the National Aeronautics and Space Administration; the observatory was made possible by the generous financial support of the W. M. Keck Foundation. The authors wish to recognize and acknowledge the very significant cultural role and reverence that the summit of Mauna Kea has always had within the indigenous Hawaiian community; we are most fortunate to have the opportunity to conduct observations from this mountain. ESO VLT data were acquired under programs 68.D-0571(A), 69.D-0438(A), and 170.A-0519(A), and La Silla data under program 68.A-0443. A.V.F.'s group is supported by the National Science Foundation through grant AST-0607485. A.C. is supported by grants P06-045-F ICM de MIDEPLAN, Basal CATA PFB 06/09, and FONDAP No. 15010003.

REFERENCES

- Appenzeller, I., Fricke, K., Fürtig, W., Gässler, W., Häfner, R., Harke, R., Hess, H.-J., Hummel, W., et al. 1998, *Messenger*, 94, 1
- Axelrod, T. S. 1980, Ph.D. thesis, Univ. California, Santa Cruz
- Bessell, M. S. 1990, *PASP*, 102, 1181
- Buzzoni, B., Delabre, B., Dekker, H., Dodorico, S., Enard, D., Focardi, P., Gustafsson, B., Nees, W., et al. 1984, *Messenger*, 38, 9
- Cappellaro, E., Mazzali, P. A., Benetti, S., Danziger, I. J., Turatto, M., Della Valle, M., & Patat, F. 1997, *A&A*, 328, 203
- Clocchiatti, A. 2002, *IAU Circ.*, 7793, 2
- Clocchiatti, A., & Prieto, J. L. 2001, *IAU Circ.*, 7781, 2
- Clocchiatti, A., Wheeler, J. C., Barker, E. S., Filippenko, A. V., Matheson, T., & Liebert, J. W. 1995, *ApJ*, 446, 167
- Dekker, H., Delabre, B., & Dodorico, S. 1986, in *Proc. SPIE Conf.*, ed. D. L. Crawford, 627, 339–348
- de Vaucouleurs, G., de Vaucouleurs, A., Corwin, H. G., Jr., Buta, R. J., Paturel, G., & Fouqué, P. 1991, *Third Reference Catalogue of Bright Galaxies* (New York: Springer)
- Evans, R. O., White, B., & Bembrick, C. 2001, *IAU Circ.*, 7772, 1
- Filippenko, A. V. 1982, *PASP*, 94, 715
- . 1988, *AJ*, 96, 1941
- . 1997, *ARA&A*, 35, 309
- Filippenko, A. V., & Chornock, R. 2002, *IAU Circ.*, 7988, 3
- Filippenko, A. V., Li, W. D., Treffers, R. R., & Modjaz, M. 2001, in *IAU Colloq. 183, Small Telescope Astronomy on Global Scales*, ed. B. Paczyński, W. P. Chen, & C. Lemme (ASP Conf. Ser. 246; San Francisco: ASP), 121
- Filippenko, A. V., Matheson, T., & Barth, A. J. 1994, *AJ*, 108, 2220
- Filippenko, A. V., Matheson, T., & Ho, L. C. 1993, *ApJ*, 415, L103
- Filippenko, A. V., & Sargent, W. L. W. 1989, *ApJ*, 345, L43
- Foley, R. J., Papenkova, M. S., Swift, B. J., Filippenko, A. V., Li, W., Mazzali, P. A., Chornock, R., Leonard, D. C., & Van Dyk, S. D. 2003, *PASP*, 115, 1220
- Fransson, C., & Chevalier, R. A. 1989, *ApJ*, 343, 323
- Horne, K. 1986, *PASP*, 98, 609
- Koribalski, B. S., Staveley-Smith, L., Kilborn, V. A., Ryder, S. D., Kraan-Korteweg, R. C., Ryan-Weber, E. V., Ekers, R. D., Jerjen, H., et al. 2004, *AJ*, 128, 16
- Li, H., & McCray, R. 1992, *ApJ*, 387, 309
- . 1993, *ApJ*, 405, 730
- Lu, N. Y., Hoffman, G. L., Groff, T., Roos, T., & Lamphier, C. 1993, *ApJS*, 88, 383
- Maeda, K., Tanaka, M., Nomoto, K., Tominaga, N., Kawabata, K., Mazzali, P. A., Umeda, H., Suzuki, T., & Hattori, T. 2007, *ApJ*, 666, 1069
- Malesani, D., Fynbo, J., Hjorth, J., Leloudas, G., et al. 2009, *ApJ*, 692, L84
- Matheson, T., Filippenko, A. V., Ho, L. C., Barth, A. J., & Leonard, D. C. 2000, *AJ*, 120, 1499
- Maund, J. R., Smartt, S. J., Kudritzki, R. P., Podsiadlowski, P., & Gilmore, G. F. 2004, *Nature*, 427, 129
- Maund, J. R., Wheeler, J. C., Patat, F., Baade, D., Wang, L., & Höflich, P. 2007a, *MNRAS*, 381, 201
- Maund, J. R., Wheeler, J. C., Patat, F., Wang, L., Baade, D., & Höflich, P. A. 2007b, *ApJ*, 671, 1944
- Mazzali, P. A., Foley, R. J., Deng, J., Patat, F., Pian, E., Baade, D., Bloom, J. S., Filippenko, A. V., et al. 2007a, *ApJ*, 661, 892
- Mazzali, P. A., Kawabata, K. S., Maeda, K., Foley, R. J., Nomoto, K., Deng, J., Suzuki, T., Iye, M., et al. 2007b, *ApJ*, 670, 592
- Mazzali, P. A., Kawabata, K. S., Maeda, K., Nomoto, K., Filippenko, A. V., Ramirez-Ruiz, E., Benetti, S., Pian, E., et al. 2005, *Science*, 308, 1284
- Mazzali, P. A., Valenti, S., Della Valle, M., Chincarini, G., Sauer, D. N., Benetti, S., Pian, E., Piran, T., et al. 2008, *Science*, 321, 1185
- Meurer, G. R., Hanish, D. J., Ferguson, H. C., Knezek, P. M., Kilborn, V. A., Putman, M. E., Smith, R. C., Koribalski, B., et al. 2006, *ApJS*, 165, 307
- Modjaz, M., Kirshner, R. P., Blondin, S., Challis, P., & Matheson, T. 2008, *ApJ*, 687, L9
- Modjaz, M., Li, W., Butler, N., Chornock, R., Perley, D., Blondin, S., Bloom, J. S., Filippenko, A. V., et al. 2009, *ApJ*, submitted (arXiv:0805.2201)
- Mould, J. R., Huchra, J. P., Freedman, W. L., Kennicutt, R. C., Jr., Ferrarese, L., Ford, H. C., Gibson, B. K., Graham, J. A., et al. 2000, *ApJ*, 529, 786
- Mulchaey, J. 2001, *LDSS-2 User's Guide* (Pasadena: Carnegie Observatories)
- Munari, U., & Zwitter, T. 1997, *A&A*, 318, 269

- Nomoto, K., Yamaoka, H., Pols, O. R., van den Heuvel, E. P. J., Iwamoto, K., Kumagai, S., & Shigeyama, T. 1994, *Nature*, 371, 227
- Oke, J. B., Cohen, J. G., Carr, M., Cromer, J., Dingizian, A., Harris, F. H., Labrecque, S., Lucinio, R., Schaal, W., et al. 1995, *PASP*, 107, 375
- Phillips, M. M., Suntzeff, N. B., Krisciunas, K., Carlberg, R., Gladders, M., Barrientos, F., Matheson, T., & Jha, S. 2001, *IAU Circ.*, 7772, 2
- Quimby, R. M., Aldering, G., Wheeler, J. C., Höflich, P., Akerlof, C. W., & Rykoff, E. S. 2007, *ApJ*, 668, L99
- Richmond, M. W., Treffers, R. R., Filippenko, A. V., Paik, Y., Leibundgut, B., Schulman, E., & Cox, C. V. 1994, *AJ*, 107, 1022
- Riess, A. G., Li, W., Stetson, P. B., Filippenko, A. V., Jha, S., Kirshner, R. P., Challis, P. M., Garnavich, P. M., et al. 2005, *ApJ*, 627, 579
- Ryder, S., Krantz, K., Sadler, E., & Subrahmanyan, R. 2001, *IAU Circ.*, 7777, 2
- Ryder, S. D., Murrowood, C. E., & Stathakis, R. A. 2006, *MNRAS*, 369, L32
- Ryder, S. D., Sadler, E. M., Subrahmanyan, R., Weiler, K. W., Panagia, N., & Stockdale, C. 2004, *MNRAS*, 349, 1093
- Sauer, D. N., Mazzali, P. A., Deng, J., Valenti, S., Nomoto, K., & Filippenko, A. V. 2006, *MNRAS*, 369, 1939
- Schlegel, D. J., Finkbeiner, D. P., & Davis, M. 1998, *ApJ*, 500, 525
- Schlegel, E. M., & Ryder, S. 2002, *IAU Circ.*, 7913, 1
- Swartz, D. A., Clocchiatti, A., Benjamin, R., Lester, D. F., & Wheeler, J. C. 1993, *Nature*, 365, 232
- Tully, R. B. 1988, *Nearby Galaxies Catalog* (Cambridge: Cambridge University Press)
- Valenti, S., Benetti, S., Cappellaro, E., Patat, F., Mazzali, P., Turatto, M., Hurley, K., Maeda, K., et al. 2008, *MNRAS*, 383, 1485
- Van Dyk, S. D., Garnavich, P. M., Filippenko, A. V., Höflich, P., Kirshner, R. P., Kurucz, R. L., & Challis, P. 2002, *PASP*, 114, 1322
- Wade, R. A., & Horne, K. 1988, *ApJ*, 324, 411
- Woosley, S., & Janka, T. 2005, *Nature Phys.*, 1, 147